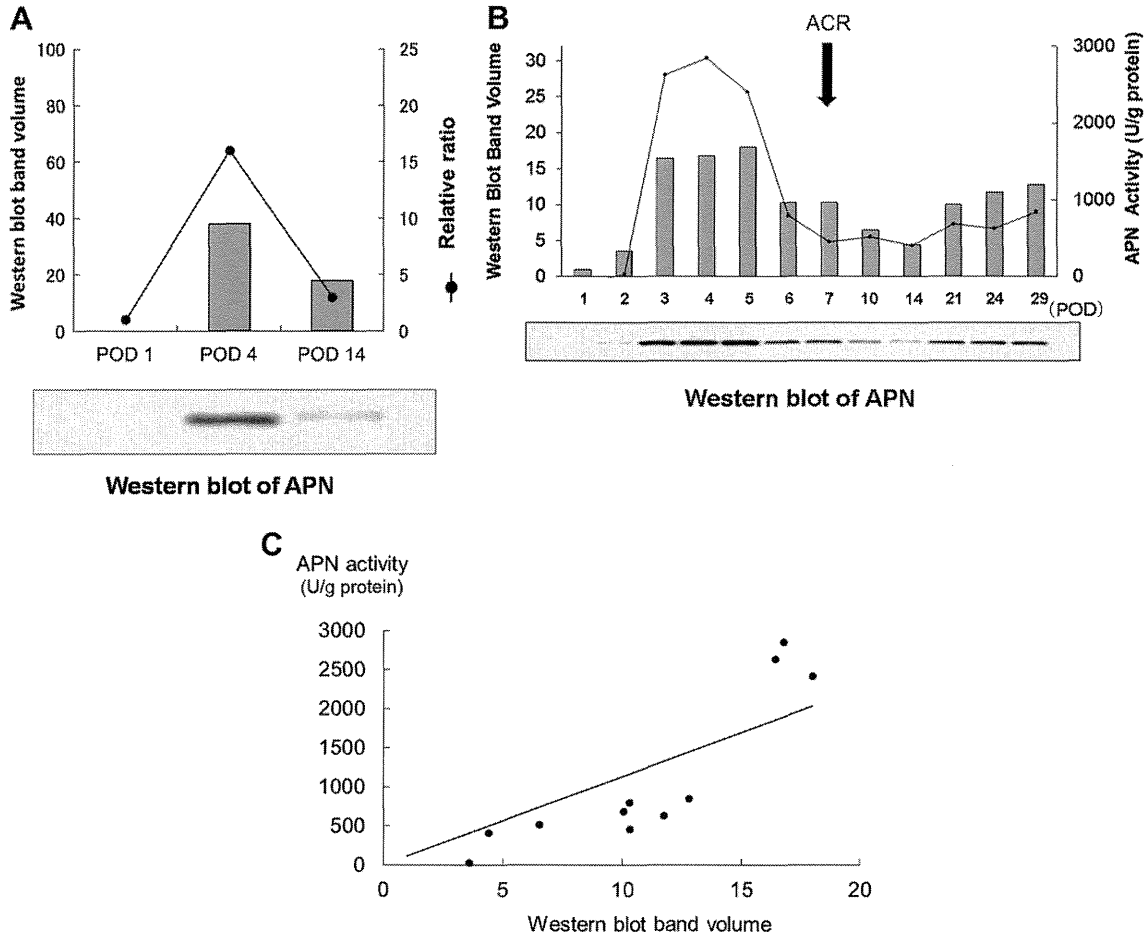

FIG. 1. Alanine aminopeptidase (APN) in bile samples. (A) APN protein expression at POD1, 4, 14 in patients with ACR. Top: Ratio of protein expression (right ordinate, ratio) based on POD1. The plot shows the relative amount of APN in bile measured by MALDI MS/MS analysis. The bar represents the Western blot band volume of APN analyzed by image software (left ordinate). Data are the amounts estimated by Western blotting and image analysis. Bottom: Western blot of APN. APN in bile increased at POD4, and then returned to the baseline. (B) Serial changes in APN activity in bile samples obtained from a single patient with ACR and measured by Western blot analysis. ACR was diagnosed at POD7. The band plot represents Western blot band volume analyzed by the image software (left ordinate) and the line plot represents APN enzyme activity (right ordinate, U/g protein). (C) Two-dimensional plot of APN enzyme activity and western blot band volume. Note the strong correlation between the two variables ($r = 0.883$, $P < 0.0001$).

determined the amount APN in the bile sample by measuring its enzyme activity, which is a simpler and easier for clinical application.

Bile APN Enzyme Activity Correlates with ACR After Liver Transplantation

Based on the inclusion criteria used in this study, recipients who were eligible for enrollment in this study were only 9 among 53 liver transplant recipients. Five of the nine recipients had biopsy-proven ACR, while the other four recipients did not have ACR (LD group). Based on the histologic diagnosis of liver biopsy, the nine recipients were classified as the ACR group ($n = 5$) and LD group ($n = 4$).

Table 2 summarizes the clinical characteristics of the nine live donors and nine liver transplant recipients. Liver biopsies at the time of donor surgery showed no fatty changes or any other histopathologic abnormalities in the nine graft livers. The cause of liver dysfunction in the LD group included small-for-size graft ($n = 1$), mild cholestasis after ABO incompatible liver transplantation ($n = 1$), and nonspecific hepatitis ($n = 2$). The bile APN enzyme activity in the nine donors was uniformly low (40.9 ± 20.1, range, 14.7–69.3 mU/mg protein).

Figure 2 shows the serial changes in APN enzyme activity in the study recipients. In the ACR group, APN activity was low after liver transplantation and, in three (60%) of five recipients of the ACR group, it gradually increased to above 500 mU/mg protein before the diagnosis of ACR, then returned to baseline after treatment of ACR with immunosuppressants and steroids. On the other hand, in two of the five recipients of the ACR group, the APN activity remained as low as that in the donor bile. In

TABLE 2

Clinical Characteristics of Recipients

	ACR cases ($n = 5$)	LD cases ($n = 4$)
Age (y) (range)	44 (19–59)	53 (40–61)
Gender (male/female)	3/2	1/3
Primary diagnosis		
HBV	1	
HBV+HCC	1	
HCV+HCC		1
Primary biliary cirrhosis	1	2
Fulminant hepatitis		1
Autoimmune hepatitis	1	
Biliary atresia	1	
Preoperative MELD score	20 (14–27)	28 (7–57)
Graft (right lobe/left lobe)	2/3	2/2
Operation time (min)	902 (642–1390)	739 (556–940)
Blood loss (mL)	3116 (1920–4400)	5800 (3350–9150)

For each variable, the mean (range) is shown.

HBV = hepatitis B virus; HCV = hepatitis C virus; HCC = hepatocellular carcinoma; ACR = acute cellular rejection; LD = liver dysfunction without ACR.

contrast, the bile APN activity remained low (<500 mU/mg protein) throughout the period in all recipients of the LD group ($n = 4$) (Fig. 2B).

Analysis of the time course of APN activity in bile of the ACR group showed that it increased 3 to 4 d before the ACR event (Fig. 2A). Therefore, APN activity within 3 d before ACR was compared with that of recipients who did not develop ACR. Available for analysis were 10 bile samples within 3 d before the ACR event and 49 bile samples outside these time periods in the ACR group ($n = 5$), while there were 47 bile samples that were not associated with ACR in the LD group ($n = 4$). APN enzyme activity in bile samples of LDLT recipients of the ACR group within 3 d before the biopsy-confirmed ACR ($n = 10$) was significantly higher (584 ± 434 U/g protein) than in bile samples of recipients free of ACR ($n = 96$, 301 ± 271 U/g protein, $P = 0.004$, Fig. 2C).

Localization of APN Along Bile Canaliculi and Its Overexpression in ACR

Immunohistochemical staining for APN in liver biopsy specimens from the donor showed APN staining in the bile canaliculi and small bile ducts. The APN expression levels in serial liver biopsy specimens from all patients of the ACR group were almost identical to that of the donor at the time of post-reperfusion, increased in the bile canaliculi and small bile ducts at ACR, then returned to the baseline after treatment of ACR and stable allograft function (Fig. 3). The lymphocyte aggregates around the portal triads did not stain for APN in the ACR group. On the other hand, the APN expression level in the LD group remained low at baseline level throughout the study period. Quantification of the immunohistochemical signal showed a significantly stronger APN staining in the ACR group at the time of ACR than all other time periods and the staining intensity in the LD group (Fig. 4).

DISCUSSION

Allograft dysfunction after liver transplantation influences post-transplant prognosis, but accurate diagnosis of this state is limited due to the risk of morbidities associated with liver biopsy and possible misinterpretation of histopathological findings. Recurrent hepatitis and ACR are often present simultaneously in clinical settings in recipients with hepatitis. Thus, it would be ideal to have an accurate, reproducible, and noninvasive method to diagnose the cause of allograft dysfunction after liver transplantation. We approached this issue previously using transcriptome analysis of liver biopsy and peripheral blood using both an animal model [19] and human samples [20, 21] and identified candidate markers associated with ACR. These studies should be continued for further validation of these candidate genes in liver and peripheral blood.

In kidney transplantation, urinary enzymes and low molecular weight proteins were reported to be useful for the diagnosis of acute rejection after the early post-transplantation phase [4–6]. The analogy of "urine" excreted from the transplanted kidney is "bile" from the allograft liver. In this study, we analyzed human bile samples using proteomic analysis to identify bile proteins that can be used as biomarkers for ACR and differentiate this condition from other causes of allograft dysfunction.

Duct-to-duct anastomosis is currently widely performed as a standard method of bile duct reconstruction in liver transplantation. Biliary drainage is quite important in order to know the amount, color, and other properties of bile output from the liver allograft as well as reducing bile duct complication [22–24]. Furthermore, it is also customary in certain cases to estimate graft function by analyzing bile bilirubin [25], bile acid [26], and other biomarkers. More importantly, bile duct reconstruction is also reported to be one of the key determinants of low morbidity in living donor liver transplantation [27, 28]. Bile is basically human waste and usually dumped without any analysis. However, it could provide a wealth of information, when another point of view is taken. The importance of biliary interleukin-6 (IL-6) in association with ACR after liver transplantation in rats [16] and deceased liver transplantation in human [17], as well as biliary ICAM-1 [8, 9] has already been reported. With this background,

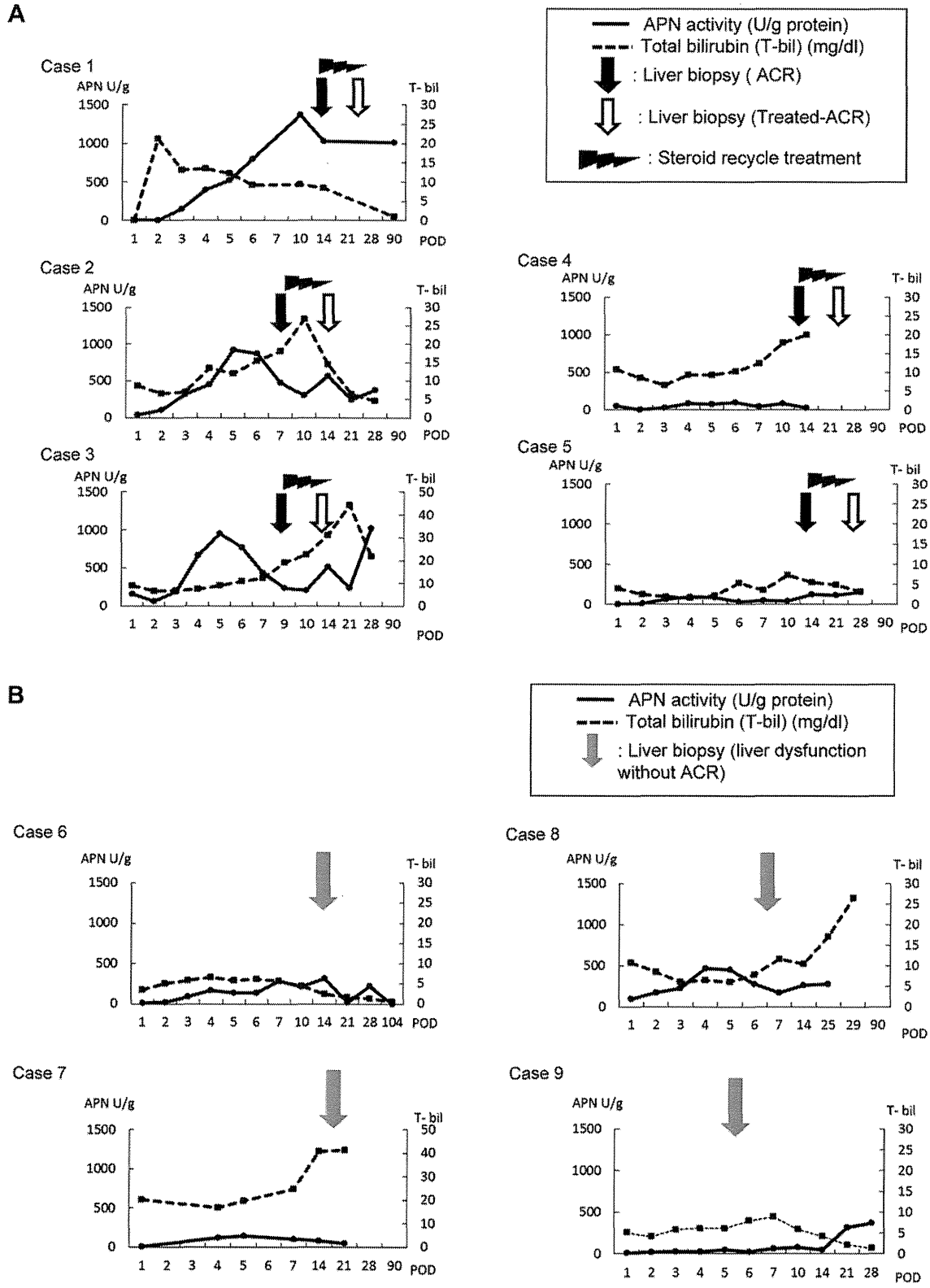

FIG. 2. Time course of biliary APN activity. (A), (B) Serial changes in biliary APN activity and serum total bilirubin level in five patients with ACR (A) and four patients with LD (B); (C) APN enzyme activity in bile samples of LDLT recipients of the ACR group within 3 d before biopsy-confirmed ACR ($n = 10$) was significantly higher than that in bile samples of patients free of ACR ($n = 96$) ($P = 0.004$). Bars indicate standard error of the mean (SEM).

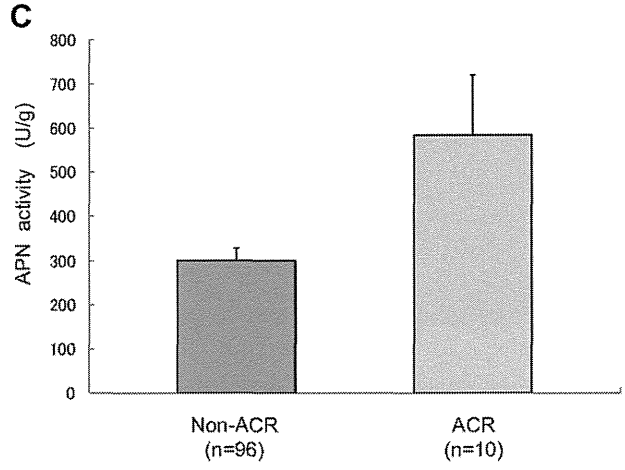

FIG. 2. (continued).

we decided to assay bile samples to determine the usefulness of bile analysis in providing clinically important information on ACR after liver transplantation.

Proteomic analysis has been used recently in the field of human clinical science such as the identification of markers for the diagnosis and/or prognosis of various malignancies [29–32]. To our knowledge, however, proteomic analysis of human bile has not yet been reported except in a limited number of studies [33, 34]. We used the technique of relative quantitative protein analysis using the ^{18}O labeling method, which allows comprehensive comparative analysis of bile proteins.

Taking this approach, we found 78 proteins that were commonly identified in all three bile samples from one recipient with ACR (obtained at POD1, 4, and 14). Among these proteins, APN (also known as CD13) was one protein whose level increased in the bile sample collected at POD4 compared with that collected at POD1 and POD14 (Fig. 1A). APN is a 150-kD transmembrane protein localized in the bile canaliculi, epithelia of the bile ducts, apical membranes of hepatocytes, mucosal cells of the gall bladder [35], peripheral blood monocytes, granulocytes [36], immature myeloid cells, epithelial cells of the intestine, synaptic membranes in the central nervous system, fibroblasts, endothelial cells, and the brush border membranes of the proximal renal tubular cells [6–8]. APN plays a pathologic role in cholelithiasis [35], biliary atresia in infants [37], and cytomegalovirus infection [38]. It was also considered as a marker of hepatocellular carcinoma, to distinguish it from metastatic tumors of the liver [39], and as a marker of cancer stem cells in hepatocellular carcinoma [40]. APN staining in the canaliculi is reported to be a highly specific marker of hepatocyte differentiation [41]. On the other hand, Jung *et al.* [4] reported that urinary APN is a significant protein associated with ACR in kidney transplantation. Surprisingly, APN was also found to correlate with liver ACR. That both bile from the liver allograft and urine from the kidney graft were linked to ACR, suggests that the mechanisms of ACR in both the liver and kidney transplants probably involve APN-related immunological and/or inflammatory processes. Further studies are necessary to establish the exact mechanism(s) of ACR, including the APN-related pathways. The amount of APN in bile detected by Western blot analysis correlated with the APN enzyme activity (Fig 1B, C). Therefore, we evaluated APN by its enzymatic activity rather than by Western blot analysis, considering its clinical applicability. Uniformly low levels of APN activity were noted in the bile samples of all donors, suggesting minimal APN activity in bile at baseline condition in the absence of liver dysfunction or ACR. Interestingly, changes in APN activity in liver transplant recipients did not correlate with other biochemical parameters such as serum bilirubin, AST, ALT, and γ-glutamyl aminotransferase (data not shown).

We classified the nine recipients into two groups; five recipients with ACR episode (ACR group) and four recipients with liver dysfunction but without ACR (LD group). We evaluated the APN activity in the patients in relation to the clinical course in both groups. As shown in Figure 2, APN activity increased above 500 mU/mg protein in a couple of days before the diagnosis of ACR in three of the five recipients of the ACR group. In contrast, APN level remained low similar to the baseline in all recipients of the LD group. Furthermore, the time course studies of APN level showed that APN increased 3–4 d before confirming the ACR by biopsy examination. Furthermore, the mean APN activity in bile samples of the LDLT recipients obtained within 3 d before ACR ($n = 10$) was significantly higher than that without ACR event ($n = 96$) ($P = 0.004$) (Fig. 2C). These results suggest that a high level of APN in the

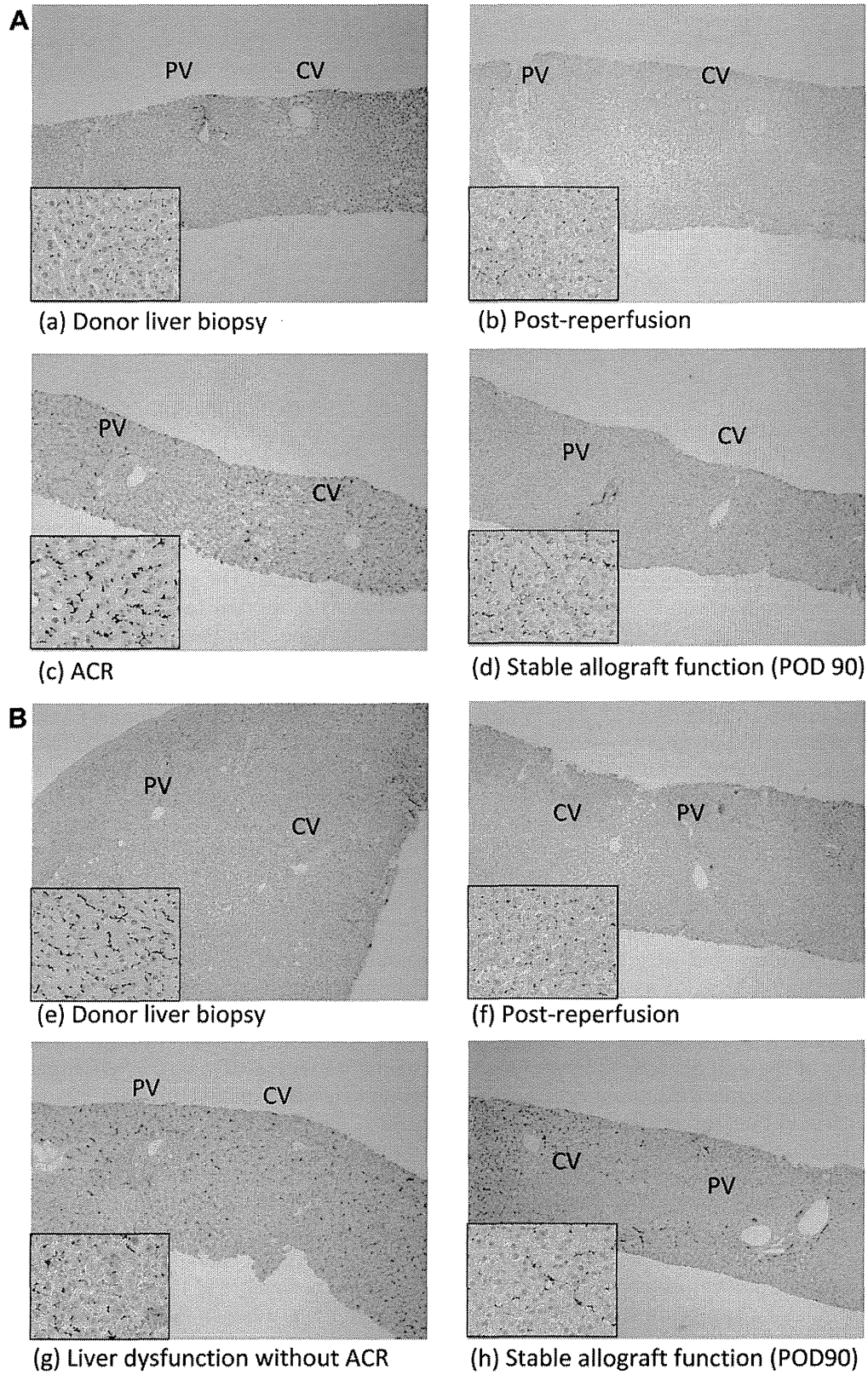

FIG. 3. Immunohistochemistry of APN in liver biopsy specimens.(A) A representative case of ACR: (a) Donor liver biopsy, (b) post-reperfusion, (c) ACR, (d) Stable allograft function (POD 90). Note the high expression of APN in patients with ACR. Note also the similarity in APN expression pattern between the donor and recipient at stable allograft function (×100, inset ×400). PV = portal vein, CV = central vein. (B) A representative case of liver dysfunction (LD): (e) Donor liver biopsy, (f) post-reperfusion, (g) liver dysfunction without ACR, (h) Stable allograft function (POD 90). Note the low APN expression compared with the patient with ACR (×400).

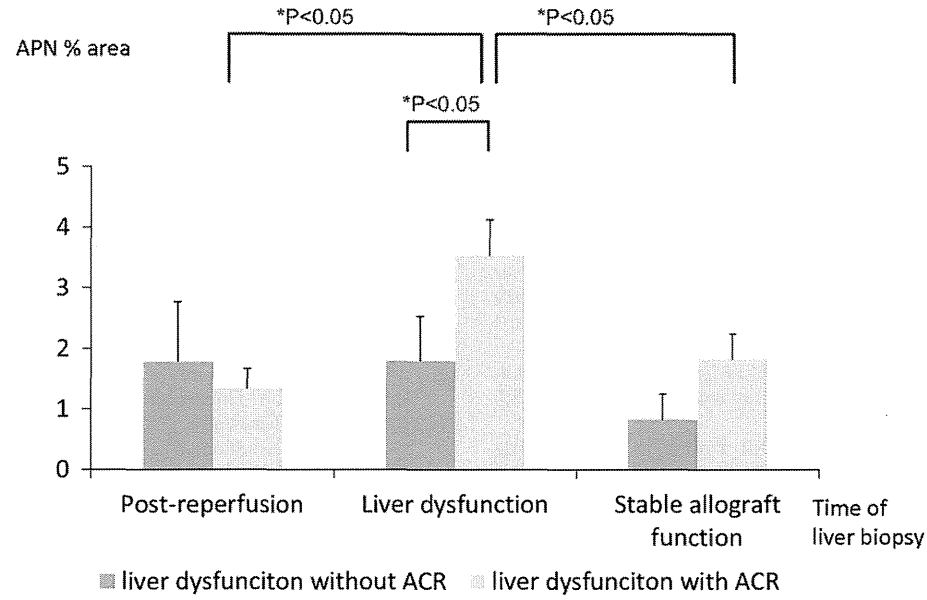

FIG. 4. Results of image analysis of APN in graft liver specimens. Data are mean ± SD of APN expression in five patients with ACR and four with LD. There was a significant difference in APN expression between the ACR and LD groups (*$P < 0.05$). The APN expression levels in liver biopsy specimens obtained 1 h after reperfusion and in the protocol liver biopsy specimens were similar, and they were significantly lower than those of the ACR group at ACR event ($P < 0.05$). Data are mean ± SD.

bile is a potentially suitable biomarker for the prediction and diagnosis of ACR.

Immunohistochemical evaluation of APN in liver biopsy samples showed the expression of APN in bile canaliculi and epithelia of the bile ducts. Furthermore, APN expression increased after liver transplantation, and such increase coincided with the confirmation of ACR by biopsy in all patients of the ACR group. Confirming the association of APN and ACR was the return of the expression level to the baseline level after treatment of ACR. In contrast, the APN expression level in recipients of the LD group did not change at all in patients with liver dysfunction as well as those with stable allograft function (Fig. 3). One possible explanation for these findings is that accumulation of active lymphocytes in the liver can induce injury of bile duct cells and, hence, can also interfere with the flow of bile stream in the bile canaliculi, which causes further injury of the bile canaliculi. This could then induce APN overexpression in the membrane of bile canaliculi cells.

The number of the recipients in this study is small, because we limited the study to recipients with confirmed histopathologic diagnosis upon liver dysfunction, excluding other recipients who had no liver biopsy, so that a definitive diagnosis could be made for liver dysfunction; ACR *versus* nonACR. Our study showed that APN level increased in the bile in association with ACR episode after liver transplantation. Furthermore, serial monitoring of APN level in the bile samples from these recipients ($n = 106$) also demonstrated increases in APN expression levels in the bile within 3 d before ACR, suggesting that biliary APN could be used as a predictor of latent and subclinical ACR, which becomes clinically apparent in the next few days. Thus, it is feasible to conclude that APN (CD13) in bile seems to be a useful and noninvasively measurable biomarker for ACR after liver transplantation.

CONCLUSION

We identified 78 proteins in bile from a liver transplant recipient by quantitative proteomic analysis based on the ^{18}O labeling method. Among these bile proteins, the expression levels of APN in bile were increased within 3 d before the development of ACR, suggesting that a high biliary APN level is a biomarker for ACR after liver transplantation.

REFERENCES

1. Maluf DG, Stravitz RT, Cotterell AH, et al. Adult living donor *versus* deceased donor liver transplantation: A 6-year single center experience. Am J Transplant 2005;5:149.
2. Liu LU, Bodian CA, Gondolesi GE, et al. Marked Differences in acute cellular rejection rates between living-donor and deceased-donor liver transplant recipients. Transplantation 2005;80:1072.
3. Shaked A, Ghobrial RM, Merion RM, et al. Incidence and severity of acute cellular rejection in recipients undergoing adult living donor or deceased donor liver transplantation. Am J Transplant 2009;9:301.
4. Jung K, Diego J, Strobelt V, et al. Diagnostic significance of some urinary enzymes for detecting acute rejection crises in renal-transplant recipients: Alanine aminopeptidase, alkaline

phosphatase, gamma-glutamyltransferase, N-acetyl-beta-D-glucosaminidase, and lysozyme. Clin Chem 1986;32:1807.
5. Kuzniar J, Marchewka Z, Krasnowski R, et al. Enzymuria and low molecular weight protein excretion as the differentiating marker of complications in the early post kidney transplantation period. Int Urol Nephrol 2006;38:753.
6. Schaub S, Wilkins JA, Antonovici M, et al. Proteomic-based identification of cleaved urinary beta2-microglobulin as a potential marker for acute tubular injury in renal allografts. Am J Transplant 2005;5:729.
7. Wittke S, Haubitz M, Walden M, et al. Detection of acute tubulointerstitial rejection by proteomic analysis of urinary samples in renal transplant recipients. Am J Transplant 2005;5:2479.
8. Adams DH, Hubscher SG, Shaw J, et al. Intercellular adhesion molecule 1 on liver allografts during rejection. Lancet 1989; 2:1122.
9. Adams DH, Mainolfi E, Elias E, et al. Detection of circulating intercellular adhesion molecule-1 after liver transplantation—evidence of local release within the liver during graft rejection. Transplantation 1993;55:83.
10. Boleslawski E, BenOthman S, Grabar S, et al. CD25, CD28 and CD38 expression in peripheral blood lymphocytes as a tool to predict acute rejection after liver transplantation. Clin Transplant 2008;22:494.
11. Bilezikci B, Demirhan B, Kocbiyik A, et al. Relevant histopathologic findings that distinguish acute cellular rejection from cholangitis in hepatic allograft biopsy specimens. Transplant Proc 2008;40:248.
12. Warle MC, Metselaar HJ, Hop WC, et al. Early differentiation between rejection and infection in liver transplant patients by serum and biliary cytokine patterns. Transplantation 2003; 75:146.
13. Ge X, Ericzon BG, Nowak G, et al. Are preformed antibodies to biliary epithelial cells of clinical importance in liver transplantation? Liver Transpl 2003;9:1191.
14. Perrella O, Sbreglia C, Arenga G, et al. Acute rejection after liver transplantation: Is there a specific immunological pattern? Transplant Proc 2006;38:3594.
15. Wang YL, Zhang YY, Li G, et al. Correlation of CD95 and soluble CD95 expression with acute rejection status of liver transplantation. World J Gastroenterol 2005;11:1700.
16. Tono T, Monden M, Yoshizaki K, et al. Biliary interleukin 6 levels as indicators of hepatic allograft rejection in rats. Transplantation 1992;53:1195.
17. Umeshita K, Monden M, Tono T, et al. Determination of the presence of interleukin-6 in bile after orthotopic liver transplantation. Its role in the diagnosis of acute rejection, Ann Surg 1996; 223:204.
18. Jung K, Scholz D. An optimized assay of alanine aminopeptidase activity in urine. Clin Chem 1980;26:1251.
19. Hama N, Yanagisawa Y, Dono K, et al. Gene expression profiling of acute cellular rejection in rat liver transplantation using DNA microarrays. Liver Transpl 2009;15:509.
20. Asaoka T, Kato T, Marubashi S, et al. Differential transcriptome patterns for acute cellular rejection in recipients with recurrent hepatitis C after liver transplantation. Liver Transpl 2009; 15:1738.
21. Kobayashi S, Nagano H, Marubashi S, et al. Guanylate-binding protein 2 mRNA in peripheral blood leukocytes of liver transplant recipients as a marker for acute cellular rejection. Transpl Int 2010;23:390.
22. Thune A, Friman S, Persson H, et al. Raised pressure in the bile ducts after orthotopic liver transplantation. Transpl Int 1994; 7:243.
23. Rabkin JM, Orloff SL, Reed MH, et al. Biliary tract complications of side-to-side without T tube versus end-to-end with or without T tube choledochocholedochostomy in liver transplant recipients. Transplantation 1998;65:193.
24. Marcos A, Ham JM, Fisher RA, et al. Single-center analysis of the first 40 adult-to-adult living donor liver transplants using the right lobe. Liver Transpl 2000;6:296.
25. Goresky CA, Gordon ER, Sanabria JR, et al. Changes in bilirubin pigments secreted in bile after liver transplantation. Hepatology 1992;15:849.
26. Hedaya MS, El Moghazy WM, Yasutomo Y, et al. Is biliary bile acid a good predictor for acute cellular rejection in living donor liver transplantation? Hepatobiliary Pancreat Dis Int 2009;8:474.
27. Kasahara M, Egawa H, Takada Y, et al. Biliary reconstruction in right lobe living-donor liver transplantation: Comparison of different techniques in 321 recipients. Ann Surg 2006;243:559.
28. Marubashi S, Dono K, Nagano H, et al. Biliary reconstruction in living donor liver transplantation: Technical invention and risk factor analysis for anastomotic stricture. Transplantation 2009; 88:1123.
29. Zhang Z, Li M, Zhang G, et al. Identification of human gastric carcinoma biomarkers by differential protein expression analysis using 18O labeling and NanoLC-MS/MS coupled with laser capture microdissection. Med Oncol 2010;27:296.
30. Roblick UJ, Bader FG, Hammarstedt L, et al. Proteomic analysis of protein expression in human tonsillar cancer: Differentially expressed proteins characterize human tonsillar cancer. Acta Oncol 2008;47:1493.
31. Ikonomou G, Samiotaki M, Panayotou G. Proteomic methodologies and their application in colorectal cancer research. Crit Rev Clin Lab Sci 2009;46:319.
32. Pitteri SJ, JeBailey L, Faca VM, et al. Integrated proteomic analysis of human cancer cells and plasma from tumor bearing mice for ovarian cancer biomarker discovery. PLoS One 2009;4:e7916.
33. Kristiansen TZ, Bunkenborg J, Gronborg M, et al. A proteomic analysis of human bile. Mol Cell Proteomics 2004;3:715.
34. Chen B, Dong JQ, Chen YJ, et al. Two-dimensional electrophoresis for comparative proteomic analysis of human bile. Hepatobiliary Pancreat Dis Int 2007;6:402.
35. Nunez L, Amigo L, Mingrone G, et al. Biliary aminopeptidase-N and the cholesterol crystallization defect in cholelithiasis. Gut 1995;37:422.
36. Chen L, Gao Z, Zhu J, et al. Identification of CD13+CD36+ cells as a common progenitor for erythroid and myeloid lineages in human bone marrow. Exp Hematol 2007;35:1047.
37. Liu C, Chiu JH, Chin T, et al. Expression of aminopeptidase N in bile canaliculi: A predictor of clinical outcome in biliary atresia and a potential tool to implicate the mechanism of biliary atresia. J Surg Res 2001;100:76.
38. Kasman LM. CD13/aminopeptidase N and murine cytomegalovirus infection. Virology 2005;334:1.
39. Rocken C, Licht J, Roessner A, et al. Canalicular immunostaining of aminopeptidase N (CD13) as a diagnostic marker for hepatocellular carcinoma. J Clin Pathol 2005;58:1069.
40. Haraguchi N, Ishii H, Mimori K, et al. CD13 is a therapeutic target in human liver cancer stem cells. J Clin Invest 2010;120:3326.
41. Lian WN, Tsai JW, Yu PM, et al. Targeting of aminopeptidase N to bile canaliculi correlates with secretory activities of the developing canalicular domain. Hepatology 1999;30:748.

Int Surg 2012;**97**:17–22

Case Report

Primary Hepatic Cancers With Multiple Pathologic Features in a Patient With Hepatitis C: Report of a Case

Go Oshima[1], Masahiro Shinoda[1], Minoru Tanabe[1], Yohei Masugi[2], Akihisa Ueno[3], Kiminori Takano[1], Minoru Kitago[1], Osamu Itano[1], Shigeyuki Kawachi[1], Kentaro Ohara[2], Masaya Oda[4], Akihiro Tanimoto[3], Michiie Sakamaoto[2], Yuko Kitagawa[1]

[1]*Department of Surgery,* [2]*Department of Pathology, and* [3]*Department of Diagnostic Radiology, Keio University, School of Medicine, Tokyo, Japan*

[4]*Internal Medicine, Sanno Hospital, Tokyo, Japan*

We report a case of multiple primary hepatic cancers exhibiting different pathologic features coexisting in a patient with chronic hepatitis C. Computed tomography showed 2 tumors in segment 8, 20 mm (S8-A) and 5 mm (S8-B) in diameter, and a 10-mm tumor in segment 6 (S6). Based on the images, the S8-A lesion was diagnosed as cholangiocellular carcinoma or combined hepatocellular carcinoma and cholangiocarcinoma (combined HCC-CC). The other 2 tumors were diagnosed as HCC. The patient underwent partial resections of segments 6 and 8. We found 2 more tumors (S8-C was 6 mm in diameter and S8-D was 4 mm) in the resected segment 8 specimen. Histopathologic examination revealed that the S8-A and S8-C tumors were combined HCC-CC, the S8-B and S6 lesions were scirrhous HCC, and the S8-D tumor was an early HCC. This is a very rare case in which different hepatic cancers with multiple pathologic features coexisted.

Key words: Multicentric hepatocellular carcinoma – Combined hepatocellular carcinoma and cholangiocarcinoma – Scirrhous type of hepatocellular carcinoma – Early hepatocellular carcinoma – Multiple pathologic features – Hepatitis C virus – Chronic hepatitis

In patients with chronic hepatitis or liver cirrhosis caused by hepatitis C (HCV) or hepatitis B virus infection, hepatocellular carcinoma (HCC) can be multicentric.[1] When liver cirrhosis is caused by HCV, the rates of occurrence and multicentricity of HCC are particularly high.[2–4] We present a very rare case in which 5 hepatic cancers composed of 4 primary cancers with 3 different types of pathologic

Reprint requests: Masahiro Shinoda, MD, Department of Surgery, Keio University, School of Medicine, 35 Shinanomachi, Shinjuku, Tokyo 160-8582, Japan.
Tel.: +81 3 3353 1211; Fax: +81 3 3355 4707; E-mail: masa02114@yahoo.co.jp

features coexisted and occurred after 10 years of sustained virologic response to HCV.

Case Report

A 67-year-old Japanese man was referred to our hospital with liver tumors in segments 6 (S6) and 8 (S8), which had been detected during a routine check-up ultrasound for hepatitis C. This patient had been treated for hepatitis C using interferon therapy 10 years earlier, which resulted in a sustained virologic response. On referral to our hospital, he had no symptoms, and physical examinations showed no abnormal findings. Laboratory data on admission were as follows: white blood cell count, 5300/mm^3; red blood cell count, 442 $\times$ 10^4/mm^3; platelet count, 16.7 $\times$ 10^4/mm^3; prothrombin time, 100%; albumin, 4.8 g/dL; total bilirubin, 0.6 mg/dL; aspartate aminotransferase, 29 IU/L; alanine aminotransferase, 28 IU/L; alkaline phosphatase, 308 IU/L; γ-glutamyl transpeptidase, 45 IU/L; cholinesterase, 406 IU/L; and indocyanine green retention rate at 15 minutes, 21.3%. Serologic analyses for viruses were as follows: hepatitis B virus surface antigen, negative; hepatitis B virus core antibody, negative; HCV antibody, positive; and HCV RNA (polymerase chain reaction), not detected. The tumor markers prothrombin induced by vitamin K absence or antagonist II (34 mAU/mL), alpha-fetoprotein (AFP, 5 ng/mL), carcinoembryonic antigen (CEA, 1.6 ng/mL), and carbohydrate antigen 19-9 (CA19-9, 10 U/mL) were all within normal limits.

Ultrasonography disclosed two hypoechoic tumors, one 10 mm in size in S6, and the other 20 mm in diameter in S8. Contrast-enhanced computed tomography (CT) revealed three tumors: one in S6 measuring 10 mm, and two in S8, measuring 5 mm and 20 mm in diameter. The 5-mm tumor in S8 showed an enhancement in the arterial phase and isodensity in the late phase (Fig. 1a and 1b). The 20-mm tumor in S8 showed a heterogeneous and peripheral enhancement in the arterial phase and no washout in the late phase (Fig. 1c and 1d). The 10-mm tumor in S6 showed an enhancement in the early phase and a washout in the late phase (Fig. 1e and 1f). Contrast-enhanced magnetic resonance imaging (MRI) with gadoxetic acid disodium (Primovist; Bayer Schering Pharma, Berlin, Germany) showed defects in the hepatobiliary phase in all tumors. Based on these imaging findings, the 5-mm tumor in S8 and the 10-mm tumor in S6 were diagnosed as typical HCC. However, the 20-mm tumor in S8 was more difficult to diagnose, and its differential diagnosis included HCC with necrotic component, metastatic tumor, cholangiocellular carcinoma (CCC), as well as combined hepatocellular carcinoma and cholangiocarcinoma (combined HCC-CC). Because upper gastrointestinal endoscopy and total colonoscopy showed no possible primary lesions, and there was also a retraction around the 20-mm tumor in S8, we narrowed down the possibilities to CCC or combined HCC-CC.

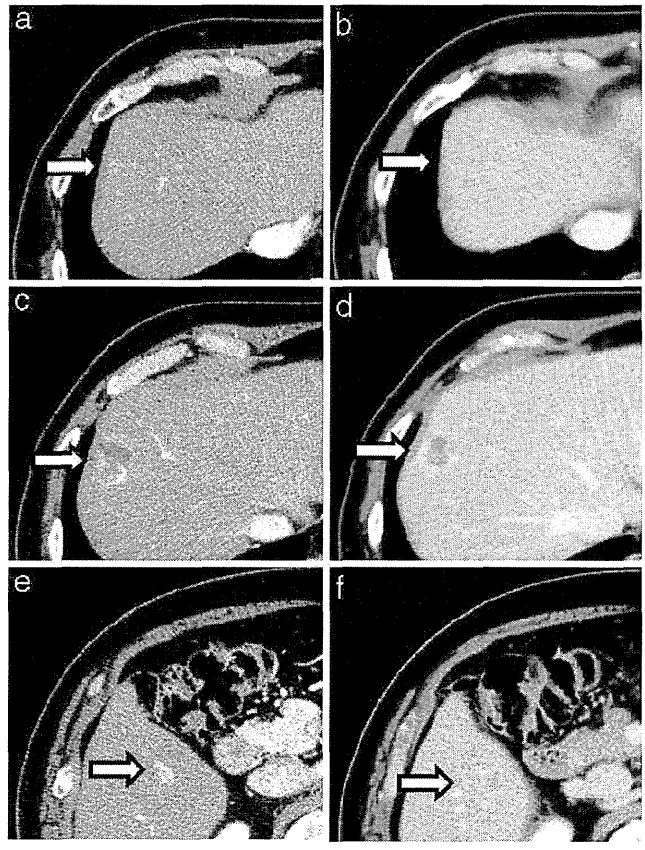

Fig. 1 Contrast-enhanced computed tomography. Three tumors were detected, measuring 5 mm (a, b) and 20 mm (c, d) in diameter in S8, and 10 mm (e, f) in S6. Early phase (a, c, and e) and late phase (b, d, and f) findings are shown. Arrows indicate tumors.

In light of these findings, we carried out partial hepatic resections of S6 and S8. The resected S6 and S8 specimens weighed 30 and 70 g, respectively. On gross examination, there were in total 5 hepatic tumors. The resected specimen of segment 6 contained a tumor, 12 mm in diameter, which showed a white lobular-shaped firm mass without capsule formation (Fig. 2a). The segment 8 specimen contained 4 tumors: 22 mm (S8-A), 10 mm (S8-B), 6 mm (S8-C), and 4 mm (S8-D) in size, all of which presented as a white firm mass without

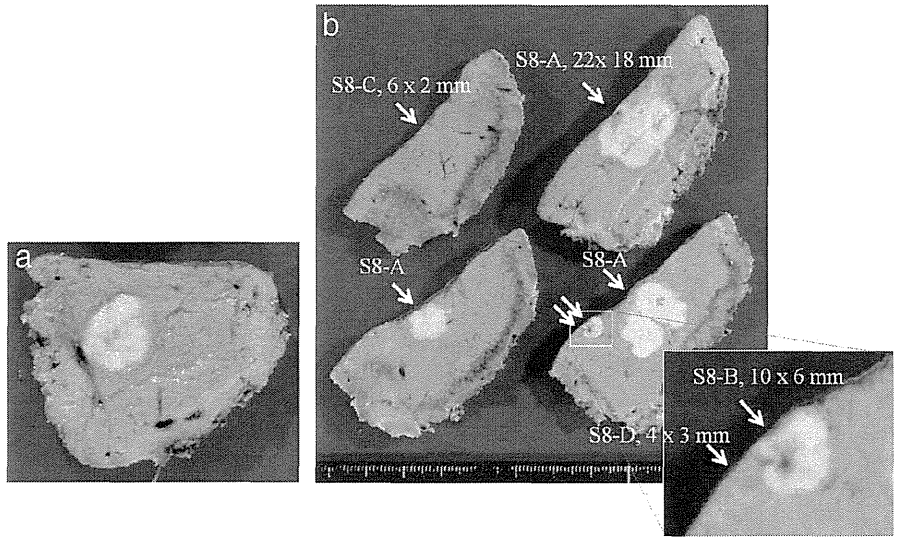

Fig. 2 Macroscopic findings of the resected specimens. The specimens of segment 6 (a) and segment 8 (b) are shown.

capsule formation (Fig. 2b). Histopathologic examination of the two tumors in S6 and S8-B revealed carcinoma cells that were arranged in an irregular moderate trabecular pattern with scirrhous growth features as characterized by fibrosis along the sinusoid-like blood spaces. This indicates that these tumors were of the scirrhous type, moderately differentiated hepatocellular carcinomas (Fig. 3a and 3b). These two scirrhous HCCs had no vascular and biliary invasions. On the other hand, the tumors in S8-A and S8-C showed two different histologic patterns and cell types that were intermixed—a hepatocellular carcinoma component composed of trabecular structures and a cholangiocellular carcinoma component made up of glandular structures with intraluminal mucin—indicating that these tumors were combined HCC-CC (Fig. 3c and 3d). The tumor in S8-A was accompanied by biliary and portal invasions. In addition, S8-D showed a vaguely nodular lesion with microscopically increased cell density. There were portal tracts within the lesion, but the tumor cells with increased nuclear cytoplasmic ratio were arranged in an irregular thin trabecular pattern and had focally invaded into the stromal tissue. Because of these findings, S8-D was considered an early hepatocellular carcinoma (eHCC) (Fig. 3e and 3f). The background liver showed mild periportal fibrosis and lymphatic infiltration, which were compatible with chronic hepatitis associated with HCV. In addition, mild pericellular and perivenular fibrosis with mild centrolobular fatty changes were observed. The locations and pathologic features of these 5 hepatic tumors are described in a schematic diagram (Fig. 4). Preoperative CT and MRI findings were retrospectively examined by 2 radiologists after pathologic examination was completed. The S8-A and S8-B tumors in the resected specimen were considered to correspond to the S8 lesions that were preoperatively detected by CT and MRI, but the S8-C and S8-D tumors in the resected specimen could not be found even by retrospective assessment of the preoperative CT and MRI images. Recurrence has not been observed at a follow-up at 15 months after the operation.

Discussion

In Japan, patients with chronic hepatitis or liver cirrhosis caused by HCV infection develop most HCCs.[1] When liver cirrhosis is caused by HCV infection, synchronous or asynchronous multiple tumors can affect the entire liver. These multiple lesions are caused by two mechanisms: intrahepatic hematogeneous tumor cell spread (intrahepatic metastasis) and *de novo* tumor development (multicentric occurrence). Although determining the carcinogenic mechanism for each tumor is difficult, in our patient, S8-C was thought to be an intrahepatic metastasis of S8-A, as the latter was microscopically accompanied by portal vein invasion, and both tumors existed closely in the same segment of the liver. On the other hand, the tumors in S6 and S8-B, both of which were scirrhous HCC, were thought to be multicentric because they showed no portal vein invasion and existed in distant segments of the liver.

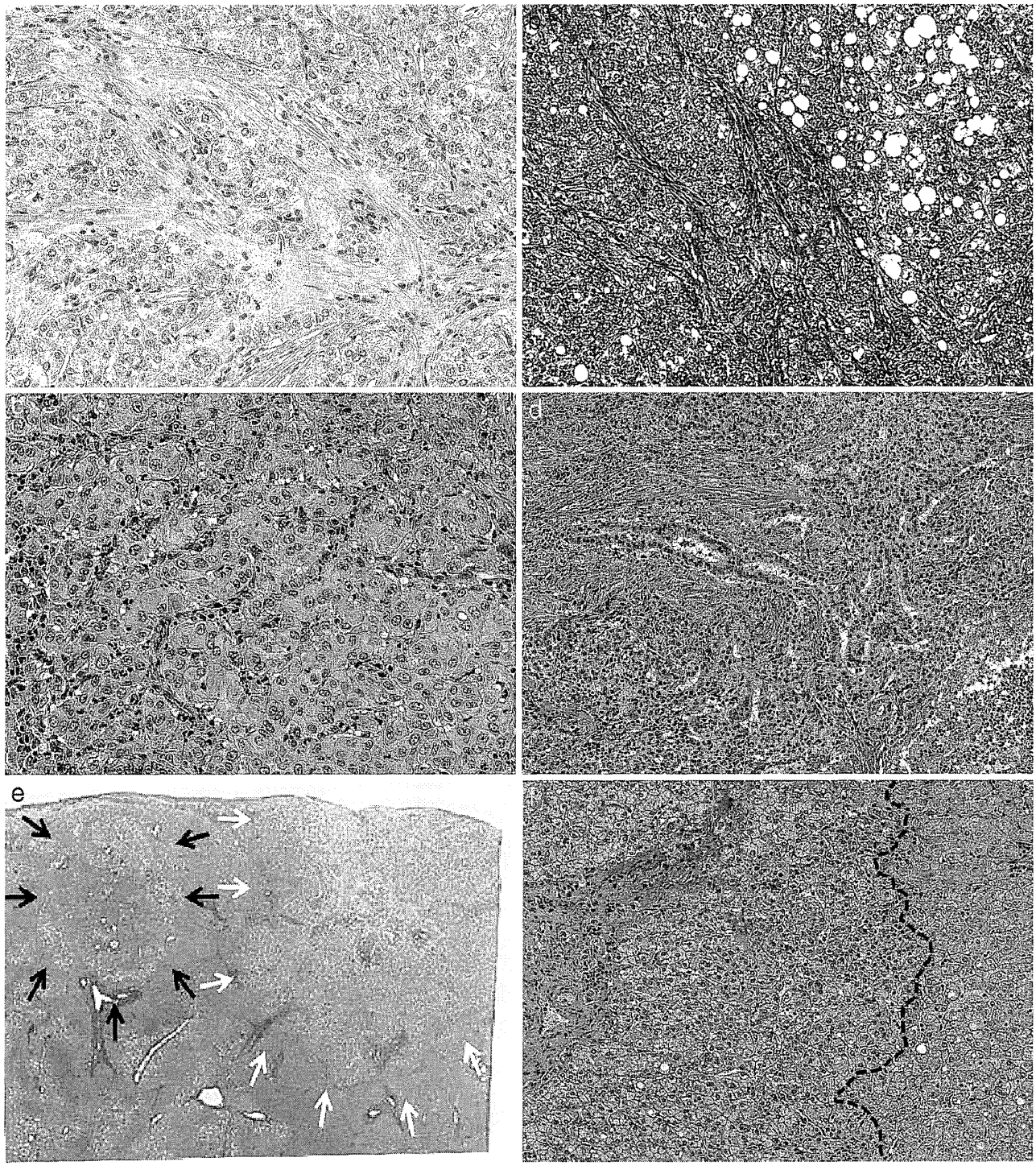

Fig. 3 Microscopic findings. The tumor in S6 was of the scirrhous type of moderately differentiated hepatocellular carcinoma (a) H&E stain (×20) (b) Azan-Mallory stain (×10). S8-A and S8-C lesions were combined HCC-CC. (c) Component of HCC (×20). (d) Component of CCC (×10). S8-B was of the scirrhous type of moderately differentiated hepatocellular carcinoma (indicated by white arrows in loupe observation [e]). S8-D was an early hepatocellular carcinoma (indicated by white arrows in loupe observation [e]). The broken line indicates a borderline between carcinoma in S8-D (left side) and normal area (right side). (f) (×15).

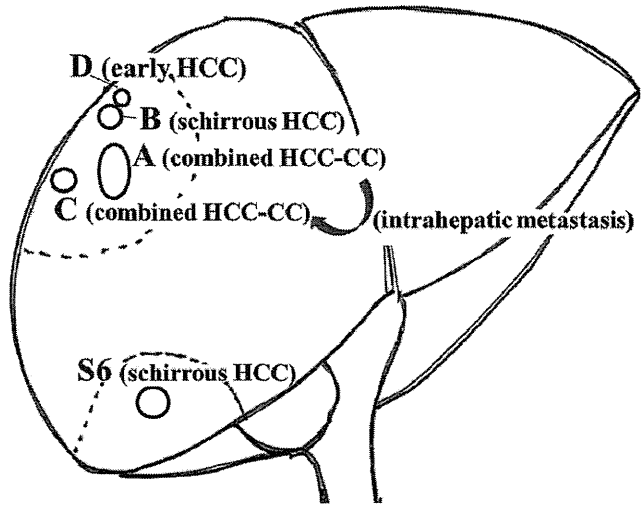

Fig. 4 Locations and pathologic features of 5 hepatic tumors.

In addition, S8-D was thought to be an eHCC. Therefore, we assume that our patient had 5 different coexisting hepatic cancers, of which 4 were primary cancers that arose multicentrically with multiple pathologic features and one was an intrahepatic metastasis.

Scirrhous HCC and combined HCC-CC are rare primary liver cancers, and in Japan, their frequencies have been reported to be approximately 4.6% and 0.54%, respectively, of primary liver cancers.[5,6] Most of the synchronous double primary hepatic cancers are a combination of HCC and CCC, and the frequency of the combination of scirrhous HCC and combined HCC-CC is extremely low. Our patient had 5 tumors, 1 combined HCC tumor with an intrahepatic metastasis, 2 scirrhous HCC-CC tumors, and 1 eHCC tumor. To our knowledge, this is the first published report of the coexistence of 5 hepatic cancers composed of 4 primary cancers with 3 different types of pathologic features in a single patient.

Accuracy and feasibility of preoperative diagnosis for primary hepatic cancers are of great interest. In our patient, 3 tumors (S6, S8-A, and S8-B) were preoperatively identified by CT and MRI, but 2 tumors (S8-C, 6 mm and S8-D, 4 mm) could not be identified, even by the retrospective assessment of the preoperative CT and MRI data. It is sometimes difficult to detect such tiny tumors using the currently available diagnostic devices. With regard to the 3 identified tumors, the preoperative diagnoses were not correct. The S6 and S8-B tumors were preoperatively diagnosed as classic HCC, but were in fact histologically a rare variant of HCC, scirrhous HCC. One of the characteristic features of scirrhous HCC is prolonged enhancement in the late phase in CT and MRI imaging,[7] but the feature varies depending on individual tumors. In addition, the finding of prolonged enhancement in the late phase is not specific to scirrhous HCC, and is frequently seen in CCC and metastatic tumors. Therefore, it is usually difficult to preoperatively diagnose scirrhous HCC. The preoperative CT findings of these 2 tumors showed early enhancement and washout (or isodensity) and were not consistent with the typical features or any features that are strongly associated with scirrhous HCC, suggesting that they were typical HCCs. We have to be aware that tumors with features that closely resemble the typical findings of HCC could also be differentially diagnosed as a rare variant of scirrhous HCC. The S8-A tumor was in fact histologically combined HCC-CC. The diagnosis of CCC or combined HCC-CC requires extra attention because additional operative procedures, such as lymph node dissection, may be necessary. However, definitive preoperative diagnosis of combined HCC-CC, in particular, seems to be challenging.[8] In our patient, although combined HCC-CC was included in the preoperative differential diagnosis of the S8-A tumor based on CT and MRI findings, we could not pinpoint the diagnosis to combined HCC-CC before surgery. Nakamura *et al*[9] hypothesized that a hypervascular tumor with high CEA and CA19-9 levels or a hypovascular tumor with a high level of AFP may indicate a preoperative diagnosis of combined HCC-CC, but these features did not correspond to our patient. Further advances in diagnostic devices or markers are needed to differentiate relatively rare hepatic cancers, such

as scirrhous HCC and combined HCC-CC, from typical HCCs.

Surgical intervention is another point of interest for primary hepatic cancers with multiple pathologic features, especially if CCC or combined HCC-CC is involved. The necessity of hilar lymph node dissection for combined HCC-CC is still under debate.[9,10] At our institute, hilar lymph node dissection is performed for preoperatively diagnosed combined HCC-CC in cases where the hilar lymph nodes appear metastatic from the preoperative imaging diagnosis or observation during surgery. In our patient, because the lymph nodes were not preoperatively and intraoperatively suspected to be metastatic, lymph node dissection was not performed. Postsurgical care, such as additional treatments including lymph node dissection or adjuvant chemotherapy, could be necessary in the future considering the possible recurrence in lymph nodes from the combined HCC-CC tumors in S8-A and S-8C. We have no immediate plans to do so because postoperative CT and serum tumor markers have not indicated any signs of recurrence at present, and we need to consider that the appearance of another tumor may not be lymph node metastasis but instead may be a multicentric occurrence of a new HCC. Considering the pathologic features of this patient, the possibility of a new HCC occurrence in the future is high. We will continue examining this patient by CT and tumor markers every 6 months so we can immediately plan the appropriate treatments for any recurrence such as lymph node metastasis or new HCC.

We reported a very rare case of 5 different coexisting hepatic cancers, whose pathologic features included scirrhous HCC and combined HCC-CC. Because of rarity and the diseases' natural characters, definite preoperative diagnoses were difficult in this patient. Special attention should always be given when encountering patients in whom unexpected tumors or whose tumor features are different from the preoperative diagnosis. The postoperative course of this patient is pathophysiologically interesting because the multiple pathologic features could have various patterns of recurrence. Considering the pathophysiologic characters of each tumor, long-term observation of the patient is necessary.

References

1. Liver Cancer Study Group of Japan. Survey and follow-up study of primary liver cancer in Japan. Report 13. *Acta Hepatol Jpn* 1999;**40**(5):288–300
2. Takano S, Yokosuka O, Imazeki F, Tagawa M, Omata M. Incidence of hepatocellular carcinoma in chronic hepatitis B and C: a prospective study of 251 patients. *Hepatology* 1995;**21**(3):650–655
3. Simonetti RG, Camma C, Fiorello F, Cottone M, Rapicetta M, Marino L *et al.* Hepatitis C virus infection as a risk factor for hepatocellular carcinoma in patients with cirrhosis. A case-control study. *Ann Intern Med* 1992;**116**(2):97–102
4. De Mitri MS, Poussin K, Baccarini P, Pontisso P, D'Errico A, Simon N *et al.* HCV-associated liver cancer without cirrhosis. *Lancet* 1995;**345**(8947):413–415
5. Kurogi M, Nakashima O, Miyaaki H, Fujimoto M, Kojiro M. Clinicopathological study of scirrhous hepatocellular carcinoma. *J Gastroenterol Hepatol* 2006;**21**(9):1470–1477
6. Ikai I, Itai Y, Okita K, Omata M, Kojiro M, Kobayashi K *et al.* Report of the 15th follow-up survey of primary liver cancer. *Hepatol Res* 2004;**28**(1):21–29
7. Kim SR, Imoto S, Nakajima T, Ando K, Mita K, Fukuda K *et al.* Scirrhous hepatocellular carcinoma displaying atypical findings on imaging studies. *World J Gastroenterol* 2009;**15**(18): 2296–2299
8. Taguchi J, Nakashima O, Tanaka M, Hisaka T, Takazawa T, Kojiro M A. Clinicopathological study on combined hepatocellular and cholangiocarcinoma. *J Gastroenterol Hepatol* 1996;**11**(8):758–764
9. Nakamura S, Suzuki S, Sakaguchi T, Serizawa A, Konno H, Baba S *et al.* Surgical treatment of patients with mixed hepatocellular carcinoma and cholangiocarcinoma. *Cancer* 1996;**78**(8):1671–1676
10. Sasaki A, Kawano K, Aramaki M, Ohno T, Tahara K, Takeuchi Y *et al.* Clinicopathologic study of mixed hepatocellular and cholangiocellular carcinoma: modes of spreading and choice of surgical treatment by reference to macroscopic type. *J Surg Oncol* 2001;**76**(1):37–46

Clin J Gastroenterol (2012) 5:189–194
DOI 10.1007/s12328-012-0296-3

CASE REPORT

Hemobilia due to biliary intraepithelial neoplasia associated with Zollinger–Ellison syndrome

Rumiko Umeda · Yuji Nakamura · Yohei Masugi · Masahiro Shinoda · Naoki Hosoe · Yoshihiro Ono · Tomonori Fujimura · Yoshiyuki Yamagishi · Hajime Higuchi · Hirotoshi Ebinuma · Shigenari Hozawa · Minoru Tanabe · Subaru Hashimoto · Michiie Sakamoto · Yuko Kitagawa · Toshifumi Hibi

Received: 30 January 2012 / Accepted: 21 March 2012 / Published online: 21 April 2012

Abstract A 58-year-old man was transferred to us from his local hospital because of failure to control his gastrointestinal bleeding by endoscopic hemostasis. Abdominal imaging suggested a hypervascular tumor of the pancreatic head (36 mm diameter), and laboratory testing showed an elevated serum gastrin level (17,800 pg/mL). Gastroduodenal endoscopy revealed multiple duodenal ulcers and active bleeding from the ampulla of Vater. The selective arterial secretagogue injection test suggested a gastrinoma in the pancreatic head, but no gastrinoma in the pancreatic tail. The patient was diagnosed with solitary pancreatic head gastrinoma complicated by hemosuccus pancreaticus, and pancreaticoduodenectomy was performed. Intraoperatively, the diagnosis was changed to primary peripancreatic lymph node gastrinoma without pancreatic involvement. The gastrointestinal bleeding stopped postoperatively and serum gastrin levels returned to normal. Histological examination of the surgical specimens revealed a small submucosal gastrinoma in the duodenum (7 mm diameter). The final diagnosis was microgastrinoma of the duodenum with peripancreatic lymph node metastasis. The cause of bleeding from the ampulla of Vater was initially obscure, but eventually a hemorrhagic erosion with moderate atypia was found in the common bile duct, indicating biliary intraepithelial neoplasia (BilIN). This is the first report of hemobilia due to BilIN with gastrinoma.

Keywords Biliary intraepithelial neoplasia · Hemobilia · Gastrinoma · Zollinger–Ellison syndrome · GI bleeding

R. Umeda · Y. Nakamura (✉) · N. Hosoe · Y. Yamagishi · H. Higuchi · H. Ebinuma · S. Hozawa · T. Hibi
Division of Gastroenterology and Hepatology, Department of Internal Medicine, School of Medicine, Keio University, 35 Shinanomachi, Shinjuku, Tokyo 160-8582, Japan
e-mail: yujinaka@a5.keio.jp

R. Umeda
e-mail: rumiko0124@z5.keio.jp

Y. Masugi · M. Sakamoto
Department of Pathology, School of Medicine, Keio University, Tokyo, Japan

M. Shinoda · Y. Ono · T. Fujimura · M. Tanabe · Y. Kitagawa
Department of Surgery, School of Medicine, Keio University, Tokyo, Japan

S. Hashimoto
Department of Diagnostic Radiology, School of Medicine, Keio University, Tokyo, Japan

Introduction

Zollinger–Ellison syndrome (ZES) was first described in 1955 by Robert Zollinger and Edwin Ellison, surgeons at Ohio State University, USA. This syndrome presents with a triad of acid hypersecretion, severe peptic ulceration, and gastrinoma (non-beta islet cell tumor of the pancreas that secretes large amounts of gastrin) [1]. ZES is rare, with an incidence of about 1 case per million people per year in the USA. Solitary lesions are located in the duodenum in 50–70 % of cases and in the pancreas in 20–40 % of cases. More than 90 % of gastrinomas are found in the anatomical triangle referred to as the gastrinoma triangle, which has vertices at (a) the confluence of the cystic and common bile ducts, (b) the junction of the second and third portions of the duodenum, and (c) the junction of the neck and body of the pancreas [2]. Duodenal gastrinomas are usually much smaller than pancreatic gastrinomas. When the primary lesion is not located in either the pancreas or the duodenum, primary lymph node gastrinoma is diagnosed.

In 2005, Zen et al. [3] proposed 3 grades of biliary intraepithelial neoplasia (BilIN) after analyzing atypical/proliferative lesions of the intrahepatic bile ducts in patients with hepatolithiasis. BilIN occurs in cases of cholelithiasis, familial adenomatous polyposis, sclerosing cholangitis, and pancreatobiliary reflux, and is categorized into 3 types (BilIN-1, low-grade; BilIN-2, intermediate-grade; and BilIN-3, high-grade/carcinoma in situ) [4]. BilIN is characterized by atypical epithelial cells with multilayering of nuclei and micropapillary projections into the lumen, and is believed to play a major role in the development of cholangiocarcinoma through a dysplasia-to-carcinoma sequence. Expression of TP53 is helpful in identifying dysplastic changes, which are more common and extensive in BilIN than in reactive epithelium.

Bleeding from the ampulla of Vater is a rare type of gastrointestinal (GI) bleeding, and can be caused by diseases of the ampulla of Vater, the pancreatic duct, or the biliary duct. Hemosuccus pancreaticus is bleeding from the pancreatic duct, pancreas, and structures adjacent to the pancreas. Hemobilia is a manifestation of hepatobiliary disease, and is most commonly caused by medical interventions such as liver surgery or by blunt abdominal trauma, and less commonly by hepatobiliary diseases such as hepatic artery aneurysm or biliary tract neoplasm. Here we report a case of ZES with active bleeding from the ampulla of Vater, which was initially diagnosed as hemosuccus pancreaticus due to pancreatic gastrinoma. After surgical resection of the structures in the gastrinoma triangle, histological examination of the resected specimens revealed microgastrinoma of the duodenum with metastasis to a peripancreatic lymph node, and a hemorrhagic erosion in the common bile duct with atypical epithelial cells indicating BilIN. Although several cases of hemobilia due to carcinoma have been reported [5, 6], this is the first report of hemobilia due to BilIN in a patient with ZES.

Case report

A 58-year-old man was transferred from his local hospital to our hospital with uncontrolled GI bleeding from multiple duodenal ulcers. He had visited his local hospital complaining of melena and faintness 10 days previously, and gastroduodenal endoscopy had revealed active bleeding from duodenal ulcers. Although he underwent two sessions to achieve endoscopic hemostasis with hemoclipping and ethanol injection, the GI bleeding continued and he required multiple blood transfusions. He had a history of watery diarrhea of undetermined cause for one year. The laboratory data obtained at our hospital are shown in Table 1. Abdominal ultrasonography (US), computed tomography (CT), and magnetic resonance imaging (MRI) showed a hypervascular mass measuring 36 × 28 mm (Fig. 1), which was reported to be suggestive of a neuroendocrine tumor in the pancreatic head. As serum gastrin level was elevated (17800 pg/mL), ZES was diagnosed. Gastroduodenal endoscopic examination revealed multiple duodenal ulcer scars, and hemoclips which had been placed at his local hospital. No active bleeding was observed from the duodenal mucosa, but fresh bleeding was observed from the ampulla of Vater (Fig. 2). We diagnosed hemosuccus pancreaticus due to pancreatic gastrinoma and explained to the patient that treatment would require resection. To determine the operability and location of the gastrinoma, angiography and the selective arterial secretagogue injection (SASI) test were performed. The SASI

Table 1 Laboratory data obtained on admission to our hospital

WBC	6,500/mL	TP	3.9 g/dL	Glu	132 mg/dL
Seg	82 %	Alb	2.2 g/dL	TG	129 mg/dL
Lymph	15 %	TB	0.3 mg/dL	HDL-C	24 mg/dL
Mono	3 %	BUN	16.1 mg/dL	LDL-C	69 mg/dL
RBC	283 × 10^4/mL	Crtnn	1.06 mg/dL	AMY	88 IU/L
Hb	8.6 g/dL	UA	7.9 mg/dL	CRP	0.02 mg/dL
Hct	27.3 %	Na	139 mEq/L	Fe	114 μg/dL
Plt	40 × 10^4/mL	K	4.3 mEq/L	TIBC	339 μg/dL
APTT	26.6 s	Cl	108 mEq/L	PTH-intact	45 pg/mL
PT	10.2 s	Ca	7.4 mg/dL	Calcitonin	30 pg/mL
PT-INR	0.97	IP	2.7 mg/dL	IRI	11 μU/mL
FNG	275 mg/dL	AST	18 IU/L	C-peptide	5.5 ng/mL
		ALT	26 IU/L	Gastrin	17,800 pg/mL
		LDH	150 IU/L		
		ALP	143 IU/L		
		γ-GTP	14 IU/L		

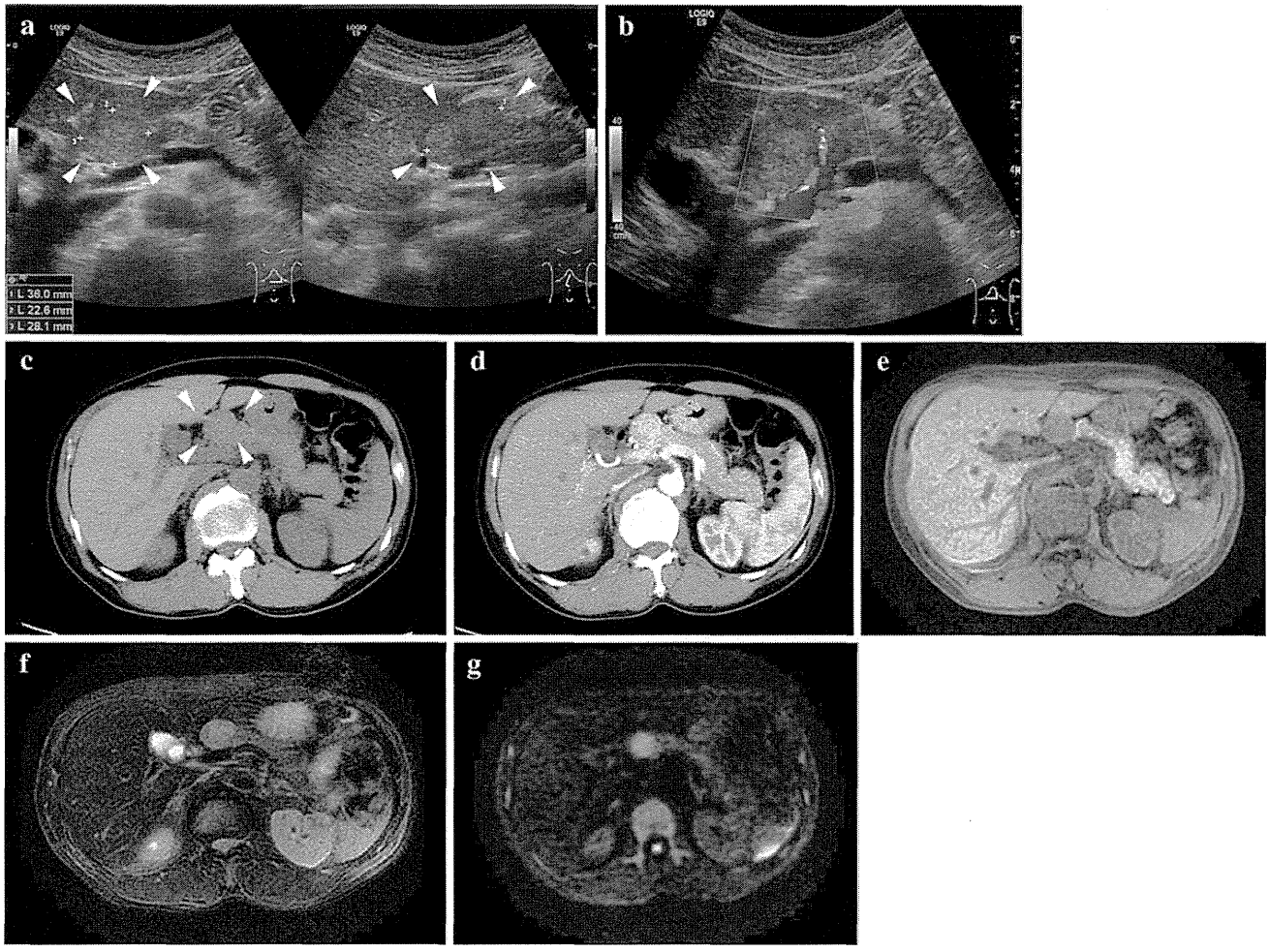

Fig. 1 Abdominal images. **a** Ultrasonography showed a hyperechoic tumor (36 × 28 mm) in the pancreatic head. **b** Doppler imaging showed a vascular signal in the mass. **c** Computed tomography showed an isodense tumor in the pancreatic head. **d** Contrast enhancement showed the vascularity of the tumor. **e** T1-weighted magnetic resonance imaging (MRI) showed a low-intensity tumor. **f** T2-weighted MRI showed a high-intensity tumor. **g** Diffusion-weighted MRI showed a high-intensity tumor. The *arrowheads* indicate the tumor

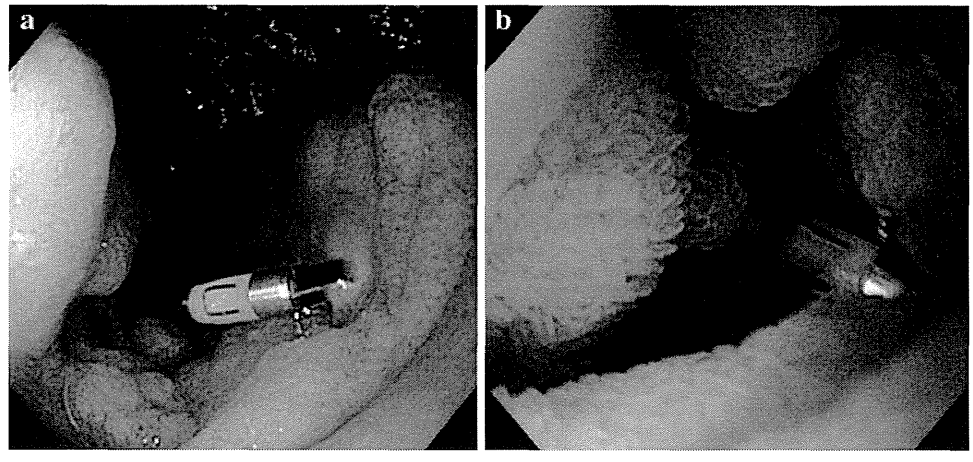

Fig. 2 Images obtained by gastroduodenal endoscopy. **a** The hemoclip which was attached to the second portion of the duodenum opposite the ampulla of Vater at the patient's local hospital. **b** Active bleeding from the ampulla of Vater

test gave positive results for celiac, superior mesenteric, and inferior pancreaticoduodenal artery injection, but negative results for splenic and transverse pancreatic artery injection (Table 2), indicating gastrinoma in the pancreatic head but not in the pancreatic tail. Pancreaticoduodenectomy was performed.

Table 2 Selective arterial secretagogue injection test (SASI) results

	0 s	30 s	60 s	90 s	120 s	180 s
CA	8,650	27,800	16,000	14,700	12,000	14,700
SMA	9,150	46,400	27,000	22,000	20,600	21,200
IPDA	10,800	61,500	31,700	26,300	26,300	18,000
TPA	9,100	8,810	10,100	12,100	95,300	11,700
SA	14,000	13,200	12,800	16,100	14,700	13,300

Blood samples were taken from the hepatic vein at 0, 30, 60, 90, 120, and 180 s after injection of calcium solution (1 mEq), and gastrin levels were measured (pg/mL)

CA celiac artery, *SMA* superior mesenteric artery, *IPDA* inferior pancreaticoduodenal artery, *TPA* transverse pancreatic artery, *SA* splenic artery

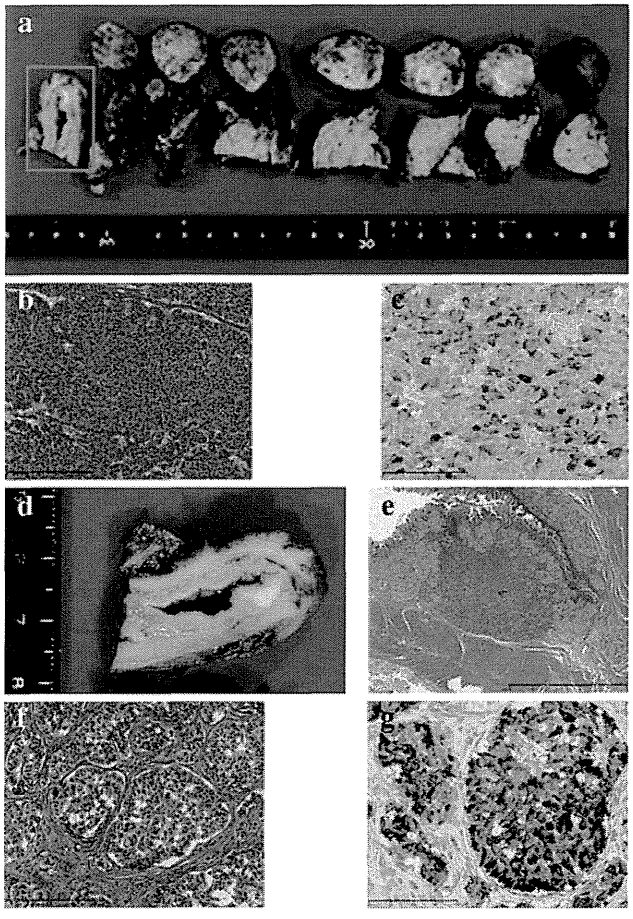

Fig. 3 Surgically excised tissues. **a** Macroscopic appearance of the excised peripancreatic tumor and the head of the pancreas. The duodenal tumor is shown in the rectangle at the *left*. **b** Microscopic appearance of the peripancreatic tumor stained with hematoxylin and eosin (H&E) (×20), showing that the tumor was a lymph node metastasis. **c** The metastatic lymph node showed positive staining for gastrin (×20). **d** Macroscopic appearance of the submucosal microtumor in the second portion of the duodenum. **e** Loupe image of the submucosal microtumor in the second portion of the duodenum. **f** Microscopic appearance of the tumor in the second portion of the duodenum stained with H&E (×20). **g** The tumor in the second portion of the duodenum showed positive staining for gastrin

Pathological examination of the excised tissues revealed that the gastrinoma was not located in the pancreas, but in a lymph node measuring 30 × 28 × 23 mm near the common hepatic artery at the head of the pancreas (Fig. 3). A small submucosal tumor (7 mm diameter) was found in the second portion of the duodenum. Immunohistochemical studies for gastrin showed the same pattern of positive staining in the duodenal tumor and in the affected lymph node. The final diagnosis was duodenal microgastrinoma with metastasis to a peripancreatic lymph node. The mitotic count was 3 per 10 high-power fields and the Ki67 index was 2–3 %, giving a World Health Organization classification of NET G2. Postoperative review of the CT, MRI, and US scans indicated that the mass detected on preoperative images was compatible with a peripancreatic tumor. Review of the angiography and SASI test results could not distinguish between pancreatic and peripancreatic tumor.

No bleeding lesions were observed in the pancreas or the ampulla of Vater, but a hemorrhagic erosion was detected in the bile duct, associated with atypical biliary epithelial cells with multilayering of nuclei and micropapillary projections into the lumen. There was an abrupt transition between the area of cellular abnormalities and the normal biliary epithelium, indicating BilIN rather than reactive changes (Fig. 4). Immunohistochemical analysis demonstrated strongly positive immunolabeling for Ki-67 and positive staining for TP53. No stromal invasion or severe atypia regarded as carcinoma was observed. The pathological change in the bile duct was diagnosed as BilIN-2/3 with hemorrhagic erosion. The gastrin level decreased back to normal postoperatively (39 pg/mL), and the patient's anemia resolved without further need for blood transfusion.

Discussion

To the best of our knowledge, this is the first report of hemobilia due to BilIN in a patient with ZES. The clinical features of hemobilia include upper abdominal pain, upper GI hemorrhage, and jaundice, and all three may be present in up to 22 % of cases [7]. Hemobilia is most commonly reported when there is a history of liver injury or

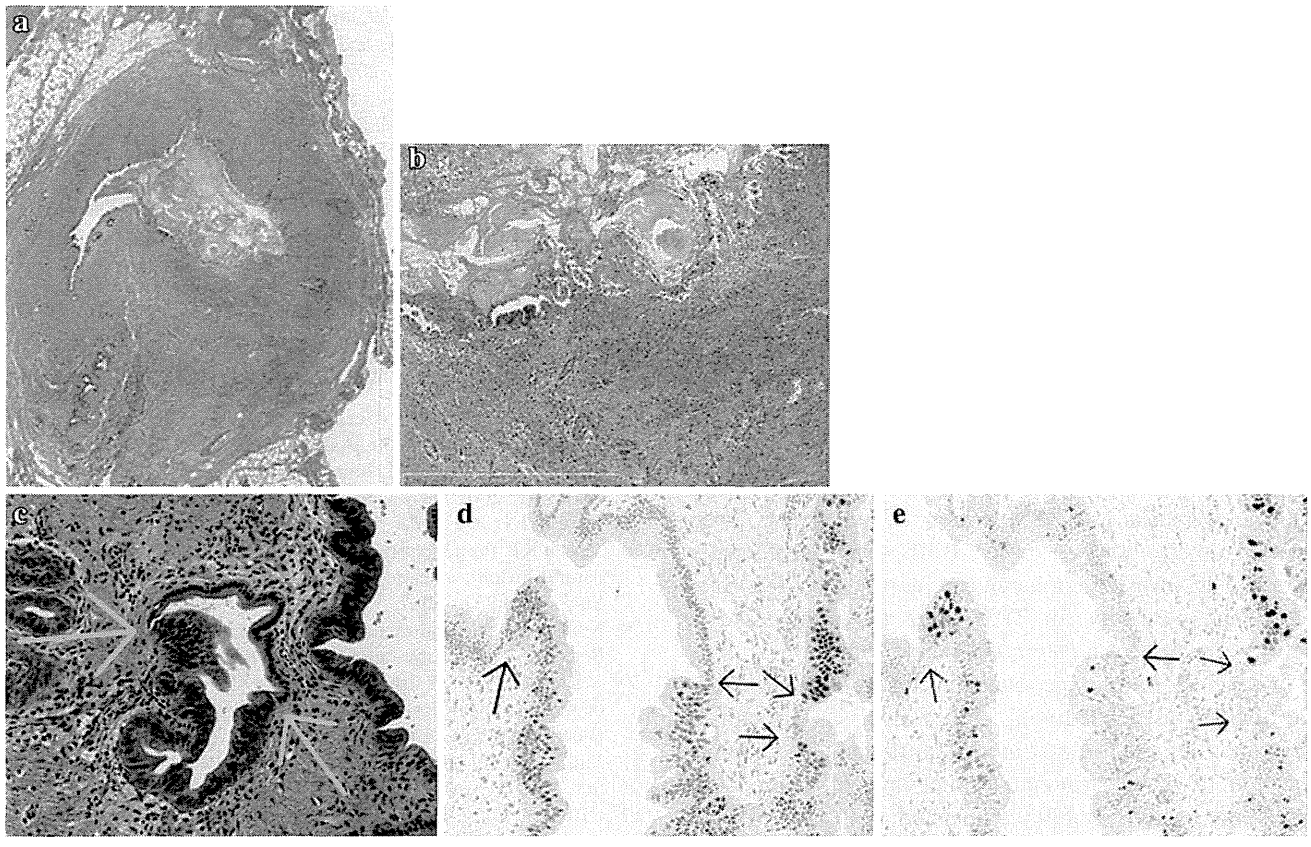

Fig. 4 **a** Loupe image of the hemorrhagic erosion in the bile duct. **b** Microscopic appearance of the hemorrhagic erosion in the bile duct (H&E staining, ×10). **c** Dysplastic biliary epithelial cells with multilayering of nuclei and micropapillary projections into the lumen (×10). The *green arrows* indicate an abrupt transition between the dysplastic and normal epithelial cells. **d**, **e** Immunostaining of serial sections for TP53 and Ki-67. The *black arrows* indicate the borders between the dysplastic and normal epithelial cells (×20)

instrumentation, such as percutaneous biliary drainage (19 % of cases), liver biopsy (13 %), or cholecystectomy (13 %). Cholangiocarcinoma is not a major cause of hemobilia and is present in only 3 % of cases. The present case had GI bleeding but no abdominal pain or jaundice. The duodenal ulceration due to ZES initially masked the hemorrhage from the biliary tract, and bleeding from the ampulla of Vater was found during endoscopic examination for recurrent duodenal ulcer bleeding.

In our patient, the initial impression was of a solitary gastrinoma in the pancreatic head with hemorrhage at the ampulla of Vater. The preoperative diagnosis was therefore hemosuccus pancreaticus due to a hypervascular gastrinoma of the pancreas. We did not perform endoscopic retrograde cholangiopancreatography or endoscopic US, because repeated blood transfusions were required to treat the anemia and it was necessary to operate as soon as possible. The multiple duodenal ulcers which had required hemoclipping also increased the risk of rebleeding during endoscopic US. However, the postoperative diagnosis was microgastrinoma of the duodenum with peripancreatic lymph node metastasis but no pancreatic invasion. Conventional imaging studies fail to identify the exact location of 80 % of microgastrinomas of the duodenum because of their small size. Postoperative review of the duodenoscopy images did not detect the primary lesion. Primary lymph node gastrinomas are not particularly rare, accounting for approximately 10 % of sporadic cases [8]. Somatostatin receptor scintigraphy (SRS), a procedure commonly used to detect duodenal gastrinomas in other countries but not currently approved for use by the Japanese Ministry of Health, Labour and Welfare, is reportedly helpful in detecting occult primary gastrinomas >10 mm in diameter. As the tumor in this case was only 7 mm it might not have been detectable by SRS. Hepatic metastasis is the most important predictor of poor survival, because the lymph nodes in the gastrinoma triangle can be removed with a standard pancreaticoduodenectomy [9]. As there were no hepatic lesions in this case, no additional therapy was given.

In our case, BilIN was associated with gastrinoma. Gastrin directly stimulates the parietal cells of the stomach to secrete hydrochloric acid, and also indirectly stimulates hydrochloric acid secretion by binding to the cholecystokinin-B receptors on the enterochromaffin cells in the stomach, thereby causing histamine release which

stimulates the parietal cells. Gastrin has also been shown to have additional functions such as stimulating pancreatic secretion and gallbladder emptying [10]. However, there are no published reports describing a relationship between gastrinoma and bile duct neoplasia. Further studies are needed to evaluate the potential biliary stress caused by gastrin oversecretion. In this case, we found an erosive hemorrhagic lesion with dysplasia in the bile duct. As BilIN is limited to the mucosal layer, it seems unlikely that it would cause bleeding. Although we tried to find a relationship between the BilIN lesion and the source of bleeding histopathologically, we were unable to find one from the excised tissues. However, there have been several reports of other mucosal lesions causing bleeding, such as gastric hyperplastic polyp [11], colon adenoma [12], and bladder dysplasia [13]. Expression of TP53 has been reported to be low in early BilIN and significantly increased in invasive cholangiocarcinoma [14]. The relatively high positivity for TP53 staining in this case is highly suspicious of a carcinomatous lesion.

In conclusion, we experienced a rare case of hemobilia due to BilIN associated with ZES, which was difficult to diagnose. Surgery for gastrinoma must include complete resection of the gastrinoma triangle by pancreaticoduodenectomy, and hemobilia associated with a bile duct neoplasm should be considered as a cause of GI bleeding that is difficult to control.

Conflict of interest The authors declare that they have no conflict of interest.

References

1. Jensen RT. Gastrinoma. In: Holzheimer RG, Mannick JA, editors. Surgical treatment. Evidence-based and problem-oriented. Munich: Zuckschwerdt; 2001.
2. Fendrich V, Langer P, Waldmann J, Bartsch DK, Rothmund M. Management of sporadic and multiple endocrine neoplasia type 1 gastrinomas. Br J Surg. 2007;94:1331–41.
3. Zen Y, Aishima S, Ajioka Y, Kage M, Kondo F, Nimura Y, et al. Proposal of histological criteria for intraepithelial atypical/proliferative biliary epithelial lesions of the bile duct in hepatolithiasis with respect to cholangiocarcinoma: preliminary report based on interobserver agreement. Pathol Int. 2005;55:180–8.
4. Bosman FT, Carneiro F, Hruban RH, Theise ND. Biliary intraepithelial neoplasia. In: WHO classification of tumors of the digestive system, 4th ed. WHO, Washington DC; 2010. p. 270.
5. Alapati R, Ibrahim MA, D'Angelo DM, Malhotra SK, Nensey YM, Salah-Eldin AA, et al. Papillary cystadenocarcinoma of the bile ducts resulting in hemobilia. Am J Gastroenterol. 1989;84:1564–6.
6. Pasos-Altamirano G, Mendieta-Zeron H, Fuentes-Luiton E. Hemobilia. A case report. Ann Hepatol. 2003;2:141–2.
7. Green MHA, Duell RM, Johnson CD, Jamieson NV. Haemobilia. Br J Surg. 2001;88:773–86.
8. Norton JA, Alexander HR, Fraker DL, Venzon DJ, Gibril F, Jensen RT. Possible primary lymph node gastrinoma: occurrence, natural history, and predictive factors: a prospective study. Ann Surg. 2003;237:650–7.
9. Norton JA. Surgical treatment and prognosis of gastrinoma. Best Pract Res Clin Gastroenterol. 2005;19:799–805.
10. Valenzuela JE, Walsh JH, Isenberg JI. Effect of gastrin on pancreatic enzyme secretion and gallbladder emptying in man. Gastroenterology. 1976;71:409–11.
11. Jain R, Chetty R. Gastric hyperplastic polyps: a review. Dig Dis Sci. 2009;54:1839–46.
12. Ciatto S, Martinelli F, Castiglione G, Mantellini P, Rubeca T, Grazzini G, Bonanomi AG, Confortini M, Zappa M. Association of FOBT-assessed faecal Hb content with colonic lesions detected in the Florence screening programme. Br J Cancer. 2011;104:1779–85.
13. Cheng L, Cheville JC, Neumann RM, Bostwick DG. Natural history of urothelial dysplasia of the bladder. Am J Surg Pathol. 1999;23:443–7.
14. Nakanishi Y, Zen Y, Kondo S, Itoh T, Itatsu K, Nakanuma Y. Expression of cell cycle-related molecules in biliary premalignant lesions: biliary intraepithelial neoplasia and biliary intraductal papillary neoplasm. Hum Pathol. 2008;39:1153–61.

Cancer Science
The official journal of the Japanese Cancer Association JCA

Direct inhibition of the transforming growth factor-β pathway by protein-bound polysaccharide through inactivation of Smad2 signaling

Yoshihiro Ono,[1] Tetsu Hayashida,[1,3] Ayano Konagai,[1] Hiroshi Okazaki,[1] Kazuhiro Miyao,[1] Shigeyuki Kawachi,[1] Minoru Tanabe,[1] Masahiro Shinoda,[1] Hiromitsu Jinno,[1] Hirotoshi Hasegawa,[1] Masaki Kitajima[2] and Yuko Kitagawa[1]

[1]Department of Surgery, Keio University School of Medicine, Tokyo; [2]International University of Health and Welfare, Tochigi, Japan

(Received June 11, 2011/Revised October 19, 2011/Accepted October 20, 2011/Accepted manuscript online October 29, 2011/Article first published online November 28, 2011)

Transforming growth factor-β (TGF-β) is involved in the regulation of cell proliferation, differentiation, and apoptosis and is associated with epithelial–mesenchymal transition (EMT). Inhibition of the TGF-β pathway is an attractive strategy for the treatment of cancer. We recently screened for novel TGF-β inhibitors among commercially available drugs and identified protein-bound polysaccharide (PSK) as a strong inhibitor of the TGF-β-induced reporter activity of 3TP-lux, a TGF-β1-responsive luciferase reporter. Protein-bound polysaccharide is used as a non-specific immunostimulant for the treatment of gastric and colorectal cancers in Japan. The anticancer activity of this agent may involve direct regulation of growth factor production and enzyme activity in tumors in addition to its immunomodulatory effect. Although several clinical studies have shown the beneficial therapeutic effects of PSK on various types of tumors, its mechanism of action is not clear. In the present study, Western blot analysis showed that PSK suppressed the phosphorylation and nuclear localization of the Smad2 protein, thereby suggesting that PSK inhibits the Smad and MAPK pathways. Quantitative PCR analysis showed that PSK decreased the expression of several TGF-β pathway target genes. E-cadherin and vimentin immunohistochemistry showed that PSK suppressed TGF-β1-induced EMT, and FACS analysis showed that PSK inhibited the EMT-mediated generation of $CD44^+/CD24^-$ cells. These data provide new insights into the mechanisms mediating the TGF-β-inhibiting activity of PSK and suggest that PSK can effectively treat diseases associated with TGF-β signaling. (*Cancer Sci* 2012; 103: 317–324)

Transforming growth factor-β (TGF-β) is involved in various biological activities, such as cell proliferation, differentiation, and apoptosis[1–3] and is also considered a major inducer of epithelial–mesenchymal transition (EMT) during development.[4,5] Inactivation of the TGF-β pathway during the early stages of carcinoma may contribute to carcinogenesis because TGF-β signaling is implicated in the negative regulation of cell proliferation.[2,6] Paradoxically, TGF-β is often overexpressed in malignant cells and alters tumor-specific cell fates and facilitates immunosuppression, deposition of ECM proteins, and angiogenesis.[7,8] Cancer cells overexpressing active TGF-β1 showed increased metastatic ability,[9] and targeting of TGF-β signaling prevented metastasis in several neoplastic tumors including breast, prostate, and colorectal cancers.[10,11] Furthermore, recent studies have suggested new roles for TGF-β signaling in the tumor microenvironment associated with the regulation of cancer stem cells and their niches.[12,13] Clinical studies have shown a positive correlation between TGF-β1 expression and metastasis and poor prognosis in gastric, breast, and colorectal carcinomas.[14–18] Thus, the inhibition of invasion and metastasis through inhibition of the TGF-β pathway could be a promising treatment strategy. However, the application of inhibitors in standard cancer therapy requires both careful evaluation of the clinical benefits and the development of effective strategies to overcome the side-effects associated with the toxicity of these agents.

A previous study suggested that protein-bound polysaccharide (PSK) modulates the biological activity of TGF-β1 and β2 by binding to their active forms.[19] Protein-bound polysaccharide obtained from *Basidiomycetes* has been used as an agent in the treatment of cancer in Asia for over 30 years.[20,21] The anticancer activity of PSK, which is derived from the fungus *Coriolus versicolor*, has been documented in experimental models *in vitro*[22] and in human clinical trials. Several randomized clinical trials have shown that PSK has anticancer potential in adjuvant cancer therapy, with positive results in the treatment of gastric, esophageal, colorectal, breast, and lung cancers.[23–26] These studies suggest that the efficacy of PSK is due to its ability to act as an immunomodulator of biological responses, but the mechanism of action of PSK has not been fully elucidated.

We recently screened for TGF-β inhibitors among commercially available drugs and identified PSK as a strong inhibitor of 3TP-lux, a TGF-β-responsive luciferase reporter. The present study investigated the inhibitory effect of PSK on the TGF-β pathway and TGF-β-induced EMT as possible mechanisms that mediate the anticancer activity of PSK.

Materials and Methods

Cell culture. The human breast epithelial cell line MCF10A was a kind gift from Dr. S. Maheswaran from the Massachusetts General Hospital Cancer Center (Charlestown, MA, USA). The human colorectal cancer cell line SW837, human pancreatic cancer cell line PANC-1, human stomach cancer cell line MKN45, human embryonic kidney cell line HEK293, and monkey kidney cell line COS-1 were obtained from ATCC (Rockville, MD, USA). The culture conditions used for the maintenance of these cell lines have been described previously.[27] Briefly, human pancreatic adenocarcinoma PANC-1, human kidney HEK293, and monkey kidney COS-1 cells were maintained in DMEM (Invitrogen, Carlsbad, CA, USA). Human mammary epithelial MCF10A cells were maintained in DMEM/F12, human gastric cancer MKN-45 cells were maintained in RPMI-1640, and human colorectal cancer SW837 cells were maintained in Leibovitz's L-15 Medium (Invitrogen). All cell culture media were supplemented with 10% FBS (BioWest,

[3]To whom correspondence should be addressed.
E-mail: tetsu@z7.keio.jp

doi: 10.1111/j.1349-7006.2011.02133.x